Proceedings of the ASME 2019 38th International Conference on Ocean, Offshore and Arctic Engineering
OMAE2019
June 9-14, 2019, Glasgow, United Kingdom

OMAE2019-95347

LOCAL BLOCKAGE EFFECTS FOR IDEALISED TURBINES IN TIDAL CHANNELS

Lei Chen
Department of Engineering Science
University of Oxford
Oxford OX1 3PJ
United Kingdom
lei.chen@eng.ox.ac.uk

Paul A. J. Bonar
School of Engineering
University of Edinburgh
Edinburgh EH9 3FB
United Kingdom
p.bonar@ed.ac.uk

Christopher R. Vogel
Department of Engineering Science
University of Oxford
Oxford OX1 3PJ
United Kingdom
christopher.vogel@eng.ox.ac.uk

Thomas A. A. Adcock
Department of Engineering Science
University of Oxford
Oxford OX1 3PJ
United Kingdom
thomas.adcock@eng.ox.ac.uk

ABSTRACT

In this paper, idealised analytical and numerical models are used to explore the potential for local blockage effects to enhance the performance of turbines in tidal channels. Arrays of turbines modelled using the volume-flux-constrained actuator disc and blade element momentum theories are embedded within one-dimensional analytical and two-dimensional numerical channel domains. The effects of local blockage on the performance of arrays comprising one and five rows of actuator discs and tidal rotors operating in steady and oscillatory channel flow are then examined. In the case of steady flow, numerical results are found to agree very well with the two-scale actuator disc theory of Nishino & Willden [1]. In the case of oscillatory flow, however, numerical results show that the shorter and more highly blocked arrays produce considerably more power than predicted by the one-dimensional two-scale theory. These results support the findings of Bonar et al. [2], who showed that under certain oscillatory flow conditions, the power produced by a partial-width tidal turbine array can be much greater than predicted by two-scale theory. The departure from theory is most noticeable in the case of five turbine rows, where the two-scale theory predicts that the maximum available power should decrease with increasing local blockage but the numerical model shows the maximum available power to increase. The effects of local blockage are found to be less pronounced for the more realistic tidal rotor than for the highly idealised actuator disc but for both models, the results show that in oscillatory flow, considerably more power is available to the shorter and more highly blocked turbine arrays.

INTRODUCTION

The task of maximising the power produced by a tidal turbine array is complicated by the need to optimise the position and operation of each turbine with respect to those of all other turbines [e.g. 3]. However, idealised theoretical models can be used to simplify this complex optimisation problem and provide valuable insights to inform array design.

Garrett & Cummins [4] used an actuator disc model to show that for a single turbine (or full-width turbine array) in volume-flux-constrained flow (meaning flow with a 'rigid lid' which does not deform in response to energy extraction), the maximum power depends on the global blockage ratio, which is defined as

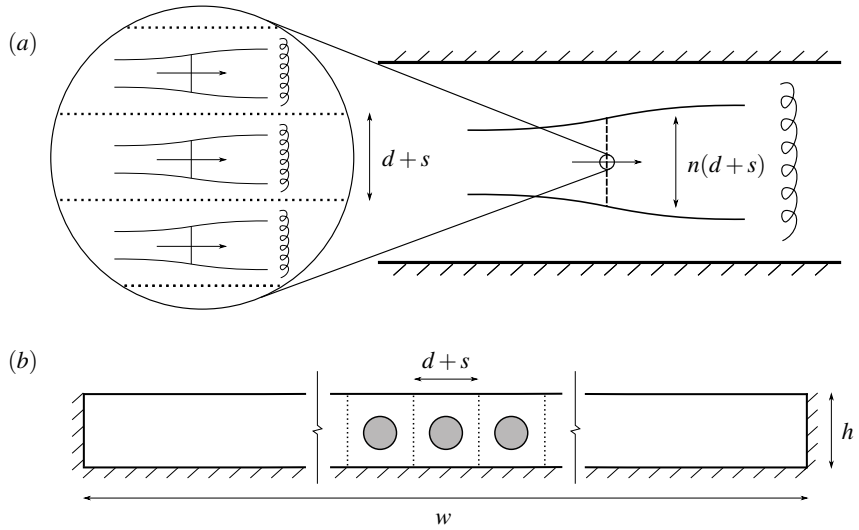

FIGURE 1: Schematic representation of the two-scale actuator disc model showing: (a) plan views of the local- (left) and array-scale (right) flows, and; (b) streamwise cross-sectional view of the partial-width tidal turbine array. Adapted from Nishino & Willden [1].

the ratio of turbine (or array) swept area to flow cross-sectional area. Nishino & Willden [1] later extended this actuator disc model to examine the maximum power that may be produced by tidal turbine arrays spanning only part of the flow cross-section. By assuming that array-scale flow events take place over much greater time and length scales than local-scale flow events, Nishino & Willden [1] were able to describe the performance of a partial-width array using a two-scale actuator disc model, comprising two loosely coupled actuator disc models used to describe the local- and array-scale flows (figure 1). Nishino & Willden [1] then showed that for each global blockage (which is now defined as the product of a local blockage and an array blockage), there exists an optimal local blockage (or equally, an optimal array blockage) which produces a peak power output. This optimal local blockage can be achieved by optimising the cross-stream spacing between the turbines within the array.

The two-scale actuator disc theory of Nishino & Willden [1] can be used to predict the optimal arrangement of, and maximum power available to, tidal turbines arranged in a single cross-stream row. However, these predictions will be limited by the simplifying assumptions underlying the theory, which include the assumption that the mass flux through the channel is unaffected by the resistance presented by the turbines. In order to predict the power available to turbines in more realistic flow conditions, the two-scale theory must first be coupled with a model of channel-scale dynamics. The simplest such model is that due to Garrett & Cummins [5], which describes the interactions between the resistance presented by the array and the bulk flow through the channel. However, a recent paper by Bonar et al. [2] has shown that under certain oscillatory flow conditions, the optimal turbine arrangement can be quite different, and the potential for enhanced power capture can be much greater than predicted by two-scale theory. Using a numerical model of actuator discs in shallow water, Bonar et al. [2] identified new two-dimensional dynamics that develop around a partial-width turbine array in oscillatory channel flow, which are not captured by these one-dimensional theories. In many cases, Bonar et al. [2] found that the optimal strategy is to group the turbines close together, so as to maximise the effects of local blockage and thereby take full advantage of these new array-scale flow dynamics.

In this paper, we extend the work of Bonar et al. [2] to consider multiple rows of turbines and a more realistic turbine representation, which is based on the volume-flux-constrained blade element momentum theory of Vogel et al. [6]. Actuator disc theory has been used extensively in analytical and numerical models of tidal stream power, and has been used to calculate upper bounds on the power available to turbines placed at candidate sites [e.g. 7], but the uniformly porous disc provides only an idealised description of turbine performance. By contrast, the more advanced blade element momentum rotor is able to better describe the forces developed by real turbine blades. These two idealised representations of tidal turbines are then embedded within two different channel domains: the one-dimensional analytical channel described by Garrett & Cummins [5], and a two-dimensional numerical channel, following Bonar et al. [2]. Different turbine arrangements are considered for both steady and oscillatory flow conditions, and the maximum available power is compared between the different channel and turbine representations. These comparisons are then used to provide a better understanding of the effects of local blockage on the performance

of turbines in tidal channels, and further assess the potential for existing theoretical models to capture these effects.

METHODS

Actuator disc model

Actuator disc theory (ADT) provides the simplest model of an axial flow turbine. The rotor plane is modelled as a uniformly porous disc which presents a resistance to the flow passing through. The classical unbounded actuator disc model has been extended to volume-flux-constrained flow by Garrett & Cummins [4], and then further extended by numerous other authors to investigate more realistic flow conditions and optimal turbine arrangements [e.g. 1; 8–11].

In ADT, turbine performance is defined by three parameters: the blockage ratio, B; the basin efficiency, η, which represents, to leading order, the ratio between the power and thrust coefficients; and the turbine tuning parameter, which is typically expressed in terms of a wake velocity coefficient (α_4 in the terminology of [8] and r_3 in the terminology of [9]). Alternatively, the tuning parameter can be expressed in terms of a local resistance coefficient, k, given by

$$k = \frac{\beta_4^2 - \alpha_4^2}{\alpha_2^2} = \frac{b_4^2 - (1-a_4)^2}{(1-a_2)^2}, \tag{1}$$

where a_2 $(= 1-\alpha_2)$ and a_4 $(= 1-\alpha_4)$ are the throughflow and wake induction factors, and α_2, α_4, and $b_4 (= \beta_4)$ are throughflow, wake, and wake bypass velocity coefficients [6; 8].

Blade element momentum rotor

A more advanced low-order turbine model is provided by blade element momentum theory (BEMT), which combines one-dimensional linear momentum theory with blade element theory to describe the forces developed by the turbine blades. The classical BEMT was derived to analyse the performance of wind turbines, and so does not account for the blockage effects which contribute significantly to tidal turbine performance [e.g. 4; 8; 12–14]. However, Vogel et al. [6] have recently extended the classical unbounded BEMT to volume-flux-constrained flow for use with tidal turbines. This blockage-corrected theory (BC-BEMT) accounts for the development of a static pressure difference in the flow passage, which enables the rotor to achieve a higher power coefficient. The BC-BEMT tidal rotor model has also been compared favourably with blade-resolved computational fluid dynamics simulations performed using different turbine blockage ratios. Further details of the derivation and validation of the BC-BEMT model are provided by Vogel et al. [6; 15].

As in ADT, the key variables for the BC-BEMT model are B, η, and the turbine tuning parameter. In BEMT, however, the wake velocity coefficients are replaced by variables more closely related to the operation of the rotor: the blade pitch angle, β, and tip speed ratio, TSR, which defines the ratio of the tangential speed of the blade tip (the product of the angular velocity of the turbine blades, ω, and rotor radius, R) to the incoming flow velocity, U_L. β and TSR may also be related through a_2, a_4, and b_4 to the resistance coefficient, k. Although BC-BEMT provides a more accurate description of turbine performance than ADT, it retains some limitations which restrict its ability to model extreme off-design conditions. For large TSR and large negative β, for instance, the tidal rotor attains a high throughflow induction factor and begins to produce non-physical flow solutions as the flow in the wake of the rotor becomes turbulent [16]. In this study, such non-physical solutions are precluded by limiting the local blockage ratio to a value ≤ 0.3125, and the tip speed ratio to a realistic range of operation: $3 \leq TSR \leq 8.5$.

Turbine performance comparisons

The performance of actuator discs and tidal rotors are compared across a range of local blockage ratios, B_L, where B_L is defined, following Nishino & Willden [1], as the ratio of turbine frontal area, $\pi d^2/4$, where d is the diameter of each of the n turbines, to the cross-sectional area of the local flow passage, $h(d+s)$, where h is the water depth and s is the cross-stream spacing between the turbines (figure 1). Schluntz et al. [14] have demonstrated the importance of designing turbines for a specific blockage ratio, but here a single tidal rotor with d = 20 m is used for convenience. Following Cao et al. [17], this rotor is designed for $U_L = 2$ m/s, $B_L = 0.16$, and $TSR = 5.5$. The blades are based on the Risø-A1-24 hydrofoil, which has been used to show good agreement between the BC-BEMT tidal rotor model and blade-resolved computational fluid dynamics simulations [17; 18].

Simulations are then used to analyse the performance of this rotor operating under three different local blockage ratios: $B_L = 0.1$, 0.2, and 0.3. The differences in performance between the tidal rotor and equivalent actuator disc are shown in figures 2 and 3, which compare the variations in C_P, C_T, and η with local resistance coefficient, k, for different values of B_L. The maximum power coefficients, $C_{P,max}$, and corresponding optimal thrust coefficients, $C_{T,opt}$, and optimal local resistance coefficients, k_{opt}, are compared in table 1. Although the variations in C_P and C_T are broadly similar, figure 2 shows that the magnitudes of C_P and C_T are much lower for the more realistic tidal rotor, which experiences both lift and drag, than for the highly idealised actuator disc [16]. Figure 3 shows that the variations in basin efficiency, η, are also quite different. The efficiency of the tidal rotor, which incorporates a number of additional energy losses, including blade tip losses, is much lower than that of the actuator disc, which is assumed to lose energy only to wake mixing. For the disc, there is a simple inverse relationship between k and η: as k increases, so does C_T and thus the amount of power

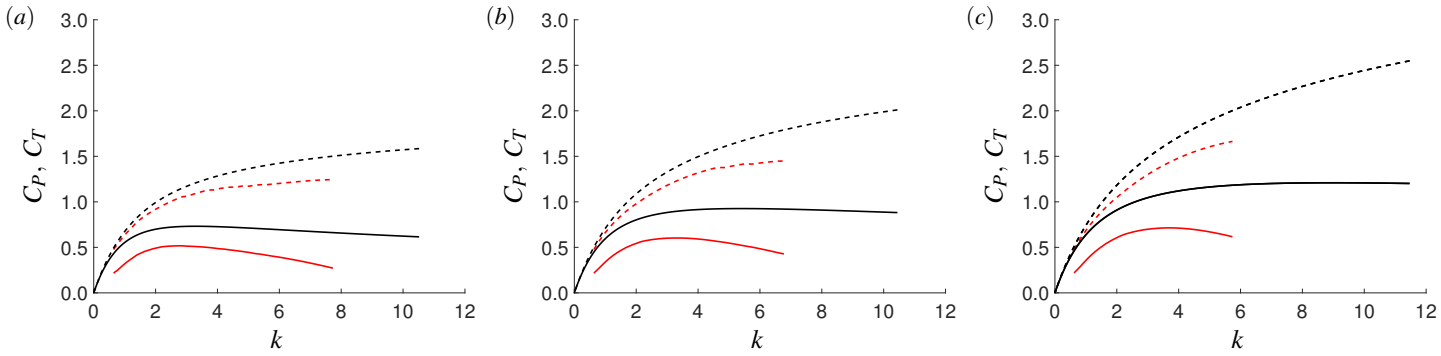

FIGURE 2: Variations in power coefficient, C_P (solid lines), and thrust coefficient, C_T (dashed lines), with local resistance coefficient, k, for an actuator disc (black lines) and tidal rotor (red lines) in: (a) effectively unblocked ($B_L = 0.01$); (b) moderately blocked ($B_L = 0.16$), and; (c) highly blocked ($B_L = 0.3$) flow. (Colour online.)

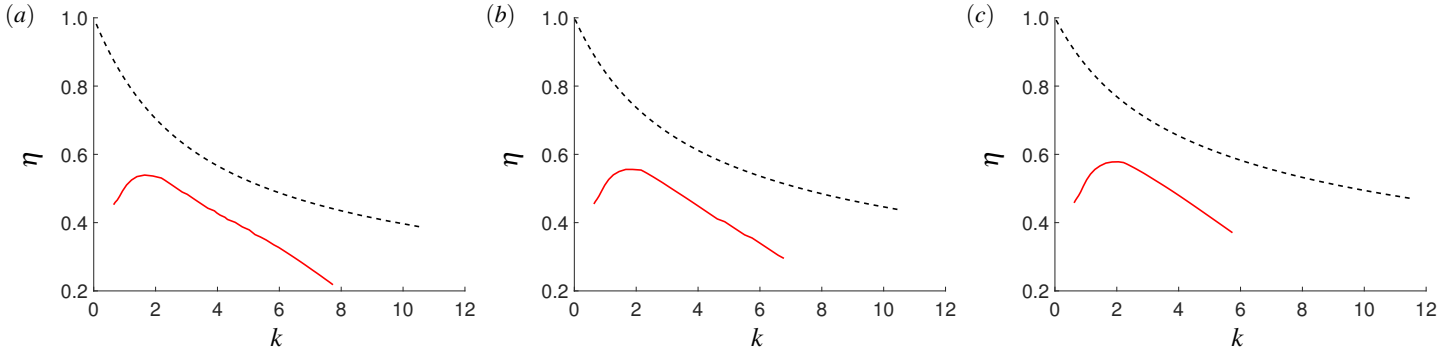

FIGURE 3: Variations in basin efficiency, η, with local resistance coefficient, k, for an actuator disc (black lines) and tidal rotor (red lines) in: (a) effectively unblocked ($B_L = 0.01$); (b) moderately blocked ($B_L = 0.16$), and; (c) highly blocked ($B_L = 0.3$) flow. (Colour online.)

dissipated in local-scale wake mixing, so η decreases. For the rotor, however, the relationship is not quite so simple: as k increases, η initially increases and then decreases as the rotor first emerges from a region of stalled flow and then cuts out as the maximum allowable TSR is achieved [16].

1D analytical channel model

Garrett & Cummins [5] proposed an idealised theoretical model to describe the extraction of energy from a simple tidal channel. In this one-dimensional theory, the tidal forcing is assumed to be unaffected by changes in the channel flow rate, and the turbine array, which is modelled as a simple opposing force, is assumed to completely span the channel width. Vennell [9] later combined this simple model with the volume-flux-constrained actuator disc theory to analyse the performance of turbine arrays spanning tidal channels.

Vennell's [9] work can be extended to consider partial-width tidal turbine arrays by replacing the volume-flux-constrained actuator disc model of Garrett & Cummins [4] with the two-scale model of Nishino & Willden [1]. Using two-scale theory, the global blockage ratio can be defined as $B_G = B_A B_L$ ($= n\pi d^2/4hw$), where w is the channel width and B_A is the array blockage, which represents the ratio between the cross-sectional area of the array, $hn(d+s)$, and the cross-sectional area of the channel, hw (figure 1). Willden et al. [19] were the first to combine the two-scale actuator disc theory of Nishino & Willden [1] with the simple channel theory of Garrett & Cummins [5] [see also 20]. Bonar et al. [2], however, were the first to show that these coupled one-dimensional models may, under certain oscillatory flow conditions, neglect leading-order physics.

2D numerical channel model

Following Bonar et al. [2], this study also employs a two-dimensional numerical channel model. This model solves the depth-averaged shallow water equations using a discontinuous Galerkin method [21; 22]. Following Draper et al. [23], the turbines are embedded within the shallow water model at sub-grid scale, and the extraction of energy is represented as a discontin-

B_L	Turbine	$C_{P,max}$	$C_{T,opt}$	k_{opt}
0.1	Rotor	0.5	1.0	2.8
0.1	Disc	0.7	1.2	3.3
0.2	Rotor	0.6	1.2	3.4
0.2	Disc	0.9	1.7	5.5
0.3	Rotor	0.7	1.4	3.7
0.3	Disc	1.2	2.4	9.2

TABLE 1: Maximum power coefficient, $C_{P,max}$, and corresponding optimal thrust coefficient, $C_{T,opt}$, and local resistance coefficient, k_{opt}, for tidal rotors and actuator discs operating with local blockages of $B_L = 0.1$, 0.2, and 0.3.

uous reduction in fluid depth. Local-scale mixing is simulated analytically, whilst array-scale mixing is simulated numerically by means of a spatially and temporally constant eddy viscosity coefficient. Though simplistic, this 'line sink' modelling approach has been found to agree with laboratory experiments of tidal energy extraction [24], and has been widely used in numerical studies of tidal stream power extraction focused on both idealised domains [e.g. 2] and real locations [e.g. 7]. The numerical code used in this study is a modified version of the DG-ADCIRC code used by Adcock et al. [7] and other authors, which has been adapted to allow the turbine properties to be specified using power and thrust curves. Further details of this modified code are provided by Schnabl et al. [25].

The numerical channel domain is 30 km long, 10 km wide, and 30 m deep. The domain is divided into 2,038 triangular elements which vary in size from 200 m around the turbine array to 1 km at the channel boundaries, and a time step of 1 s is specified. Results obtained using the present grid are found to agree to within 1% with those obtained using twice and half as many numerical elements, which indicates that the computational grid has converged. Estimates of undisturbed channel flow rate and power produced by the full-width turbine array are then found to agree to within 1% with predictions from the respective analytical models [5; 9]. The channel walls are assigned slip boundary conditions, and a realistic bed roughness coefficient is selected: $C_d = 0.002$ [26]. Steady flow is driven by assigning a constant flow rate of 1 m/s at the model inlet. This boundary condition is not entirely representative of real tidal currents but is used to facilitate comparison with the two-scale actuator disc theory, which assumes that the mass flux through the channel is unaffected by turbine resistance [1]. Oscillatory flow is driven by varying the water level at the model inlet sinusoidally, with amplitude 0.2 m and period, T = 12.42 h. In each case, the model is allowed to 'spin up' for 2 days, during which time the flow stabilises. The simulations are then allowed to continue for a further 8 days before the results from the last two complete tidal cycles are extracted and time-averaged for analysis.

RESULTS & DISCUSSION

Analytical and numerical methods are now used to explore the potential for local blockage effects to enhance the performance of turbine arrays comprising one and five rows of actuator discs and tidal rotors in steady and oscillatory channel flow. A constant global blockage of $B_G = 0.1$ is specified, and simulations are performed using eight different combinations of array width, B_A, and local blockage, B_L. Beginning with a full-width turbine array ($B_L = 0.1, B_A = 1$), B_L is then increased (and B_A reduced so that $B_G = B_A B_L$ remains constant) to a value of 0.3125 (which corresponds to an array blockage of $B_A = 0.32$). The value of the local resistance coefficient, k, is held constant in time and then varied to obtain the maximum time-averaged available power, $P_{av(max)}$. Time-varying turbine tunings [e.g. 27] will be considered in future work. Array performance is measured in terms of $P_{av(max)}$ for oscillatory flow, and for steady flow in terms of the optimal global power coefficient, $C_{PG(opt)}$, which is defined as the ratio of maximum available power to channel-scale kinetic energy flux.

Steady flow

Figures 4 and 6 show the variations in $C_{PG(opt)}$ and k_{opt} with B_L for one and five rows of actuator discs and tidal rotors. Figure 5 normalises the variations in $C_{PG(opt)}$ by the values obtained for full-width arrays ($B_L = 0.1$) in order to isolate the effects of local blockage on array performance. The figures show very good agreement between the analytical and numerical models, for both actuator discs and tidal rotors and for both one and five rows of turbines. Small differences are apparent for both small and large B_L, which are most likely due to the different assumptions underlying the two channel models, but, as noted by Perez-Campos & Nishino [28] and Bonar et al. [2], the two-scale theory is found to predict quite well the results of the numerical model.

It is also clear that although the highly idealised actuator disc tends to overestimate the performance of the more realistic tidal rotor, both turbine models respond similarly to increasing B_L. For both discs and rotors, $C_{PG(opt)}$ is shown to increase with B_L for $N = 1$ and decrease with B_L for $N = 5$. This finding shows that, as is consistent with existing work [10; 29], the effects of increasing local blockage vary with the number of turbine rows. To understand the different variations in $C_{PG(opt)}$ with B_L, it is useful to consider the corresponding variations in optimal local resistance coefficient, k_{opt} (figure 6). For $N = 1$, k_{opt} increases with increasing B_L as the greater confinement of flow enables higher optimal thrusts, but for $N = 5$, k_{opt} decreases with

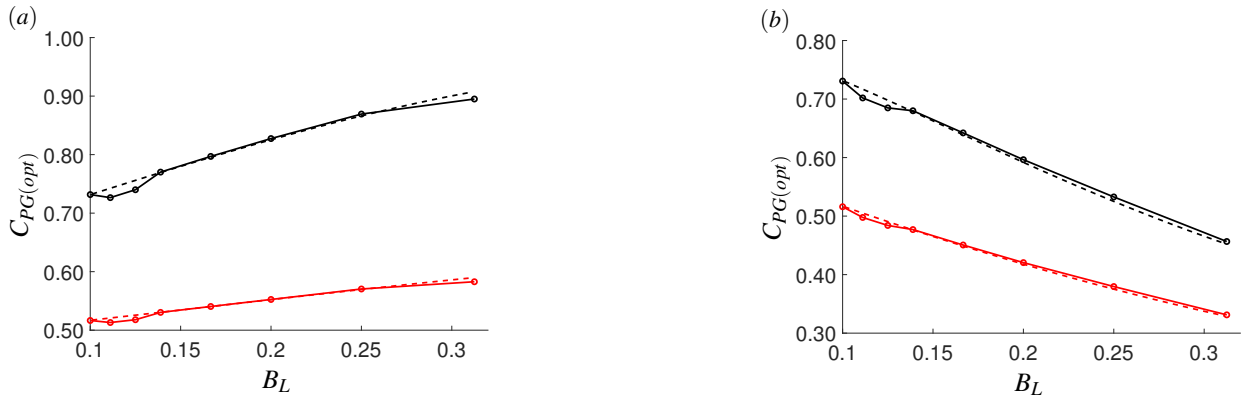

FIGURE 4: Numerically (solid lines connecting dots) and analytically (dashed lines) predicted variations in optimal global power coefficient, $C_{PG(opt)}$, with local blockage, B_L, for: (*a*) one row, and; (*b*) five rows of actuator discs (black) and tidal rotors (red) in steady flow. (Colour online).

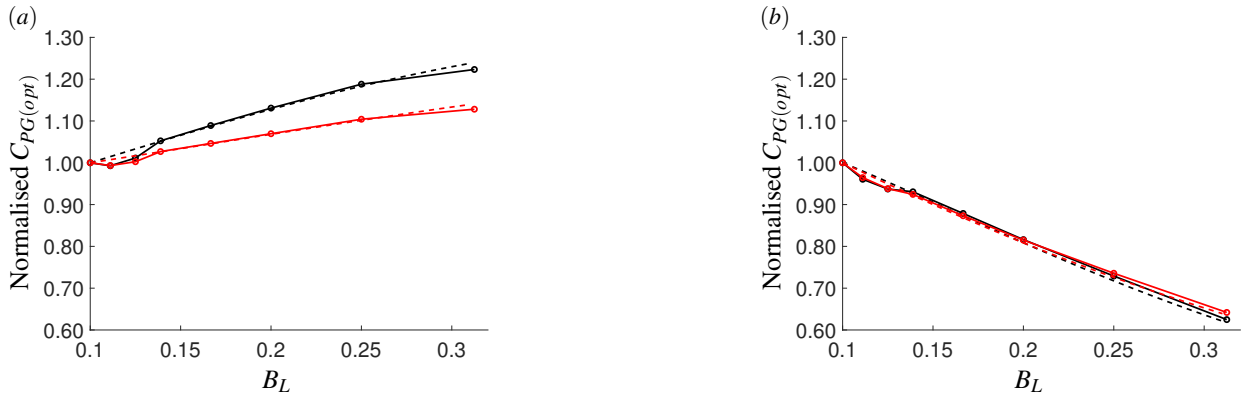

FIGURE 5: Numerically (solid lines connecting dots) and analytically (dashed lines) predicted variations in the potential for optimal global power coefficient, $C_{PG(opt)}$, enhancement with local blockage, B_L, for: (*a*) one row, and; (*b*) five rows of actuator discs (black) and tidal rotors (red) in steady flow. (Colour online.)

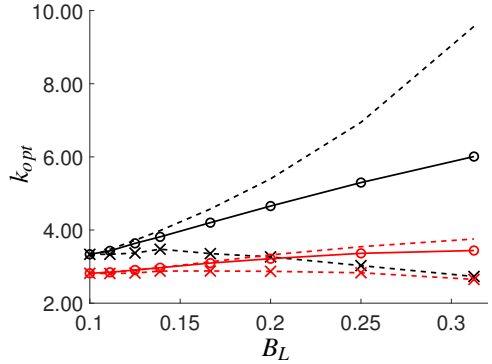

FIGURE 6: Variations in numerically (solid lines) predicted optimal local resistance coefficient, k_{opt}, for one row (circles) and five rows (crosses) of actuator discs (black) and tidal rotors (red) in steady flow. Dashed lines show the corresponding variations for the individual turbines. (Colour online.)

increasing B_L as a means by which to compensate for the much higher resistance presented by the array.

Figure 4 also shows that for both $N = 1$ and 5, the performance of the tidal rotors is less sensitive to the effects of local blockage than the actuator discs. This too may be explained by considering the corresponding variations in k_{opt} (figure 6). For both $N = 1$ and 5, the value of k_{opt} is shown to be lower and undergo less variation with B_L for the rotor than for the disc [16]. This is because, for the rotor, the peak C_P coincides with lower values of k and C_T (table 1), which limits its performance as the optimal array thrust increases. For an isolated turbine, for instance, increasing B_L from 0.1 to 0.3 results in a $\sim$70% increase in $C_{PG(opt)}$ for the disc but only a $\sim$40% increase for the rotor (table 1). Conversely, when the optimal array thrust reduces, the corresponding reduction in k_{opt} is lower for the rotor because it presents a lower resistance and thus requires a smaller tuning correction. For $N = 5$, for instance, increasing B_L from 0.1 to 0.3

results in an $\sim$18% decrease in k_{opt} for the disc but only a $\sim$5% decrease for the rotor (figure 6). Moreover, below a certain value of k, η begins to reduce for the rotor but not the disc (figure 2), which limits the performance of the rotor as k_{opt} decreases. For a given change in B_L, then, k_{opt} is shown to vary less for the more realistic rotor than for the highly idealised disc.

Figure 6 shows that the difference in k_{opt} between the rotor and disc increases with increasing B_L, as the potential for the highly idealised disc to produce relatively more power increases and the more realistic rotor experiences relatively greater energy losses. Figure 6 also shows (as dashed lines) the variations in k_{opt} which produce the maximum power coefficient for each turbine in isolation. As expected, these curves do not match the variations which produce $C_{PG(opt)}$ (which is the global power coefficient corresponding to $P_{av(max)}$, rather than the maximum global power coefficient) for the partial-width turbine arrays ($B_L > 0.1$). This is because tuning the turbines to produce the maximum power coefficient (rather than the maximum available power) would mean a significantly higher combined thrust, more flow being diverted around the array, and less power being produced as a result [e.g. 9].

For $N = 1$, the actuator disc overestimates the performance of the tidal rotor by a greater amount when B_L is large, and by a lesser amount when B_L is small, whilst the opposite is true for $N = 5$ (figures 4 and 5). Again, this may be explained by considering the corresponding variations in k_{opt}. For $N = 1$, k_{opt} increases with increasing B_L because, for a single row of turbines, $C_{PG(opt)}$ (and hence $P_{av(max)}$) may be increased by increasing the array thrust. For $N = 5$, however, k_{opt} decreases with increasing B_L because, for five rows of turbines, the applied thrust is sufficiently large that $C_{PG(opt)}$ can only be increased by applying a lower array thrust. The above finding is explained, then, by the realisation that when k_{opt} is small, the more realistic rotor is able to match more closely the performance of the highly idealised disc (figures 2 and 3).

Oscillatory flow

Figures 7 and 9 show the variations in $P_{av(max)}$ with B_L for one and five rows of actuator discs and tidal rotors operating in oscillatory flow. Figure 8 normalises the variations in $P_{av(max)}$ by the values obtained for full-width arrays ($B_L = 0.1$). As compared to the results from the steady flow simulations, it is clear that the two-scale theory is no longer able to predict well the results of the numerical model. Figure 8 shows that in oscillatory flow, the partial-width turbine arrays ($B_L > 0.1$) are shown to yield considerably more power than the equivalent full-width arrays ($B_L = 0.1$). Moreover, the trends suggest that turbine arrangements with higher B_L than those considered here can produce even more power. These findings are consistent with the work of Bonar et al. [2], who provide a detailed description of the two-dimensional array-scale dynamics underlying this significant increase in power production. The departure from theory is most noticeable for $N = 5$ (figure 8b), where the two-scale theory predicts that $P_{av(max)}$ should decrease with increasing local blockage but the numerical model shows $P_{av(max)}$ to increase.

In the case of steady flow, Nishino & Willden [1] showed that the partial-width turbine array divides the channel-scale flow into array-scale core and bypass flows. In the case of oscillatory flow, Bonar et al. [2] found that these array-scale flows oscillate side-by-side but with their peak velocities separated by a phase difference. Using a two-dimensional numerical model, Bonar et al. [2] then showed that this phase difference results in the cross-stream diversion of array-scale bypass flow through the array each time the flow changes direction, and that under certain oscillatory flow conditions, this 'reversal boost' mechanism can enhance considerably the power available to short and highly blocked turbine arrays. Naturally, however, this two-dimensional phenomenon cannot be captured using the existing one-dimensional theories, which explains the large differences in power observed for large B_L.

Whereas in steady flow, the thrust from the turbines should be carefully calibrated so as to slow but not choke the flow through the array, in oscillatory flow, it may be more beneficial to apply a larger thrust so as to maximise the effects of this new two-dimensional dynamic [2]. Figures 7 and 8 show that the potential benefits of this turbine arrangement and tuning strategy apply not only to a single row of turbines but also to five rows, and not only to actuator discs but also to tidal rotors. Comparing between the two different turbine models, it is clear that the discs again overestimate the performance of the rotors, but that the performance of the more realistic array can also be enhanced considerably by arranging and tuning the turbines to maximise the effect of this 'reversal boost'. Increasing B_L from 0.1 to 0.3125, for instance, provides $\sim$10% more power for the rotor (as compared to $\sim$20% more for the disc) when $N = 5$, and almost $\sim$35% more power for the rotor (as compared to almost $\sim$60% more for the disc) when $N = 1$.

Figure 9 shows that the considerable increases in power at large B_L are obtained by tuning the discs and rotors to apply much higher values of k_{opt} for $N = 1$, but slightly lower values of k_{opt} for $N = 5$ so as to compensate for the much higher resistance presented by the array. In steady flow, where the effects of array-scale diversion are detrimental to power production, figure 6 shows that the turbine tunings which maximise the power available to the array (solid lines) are quite different to those which maximise the power coefficient of the individual turbine (dashed lines). In oscillatory flow, however, figure 9 shows that these two different sets of optimal tunings align more closely, because the power available to the array is typically enhanced by tuning the turbines to present a higher resistance to the incoming flow so as to maximise the effect of the 'reversal boost' [2]. As in the case of steady flow, k_{opt} is generally found to be lower and undergo less variations with B_L for the more realistic rotor than the highly

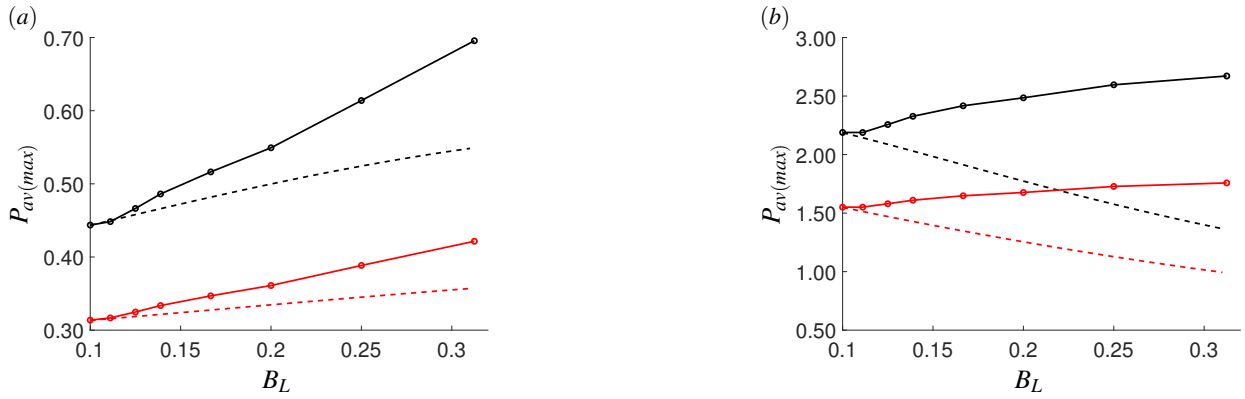

FIGURE 7: Numerically (solid lines connecting dots) and analytically (dashed lines) predicted variations in maximum available power, $P_{av(max)}$, with local blockage, B_L, for: (*a*) one row, and; (*b*) five rows of actuator discs (black) and tidal rotors (red) in oscillatory flow. (Colour online).

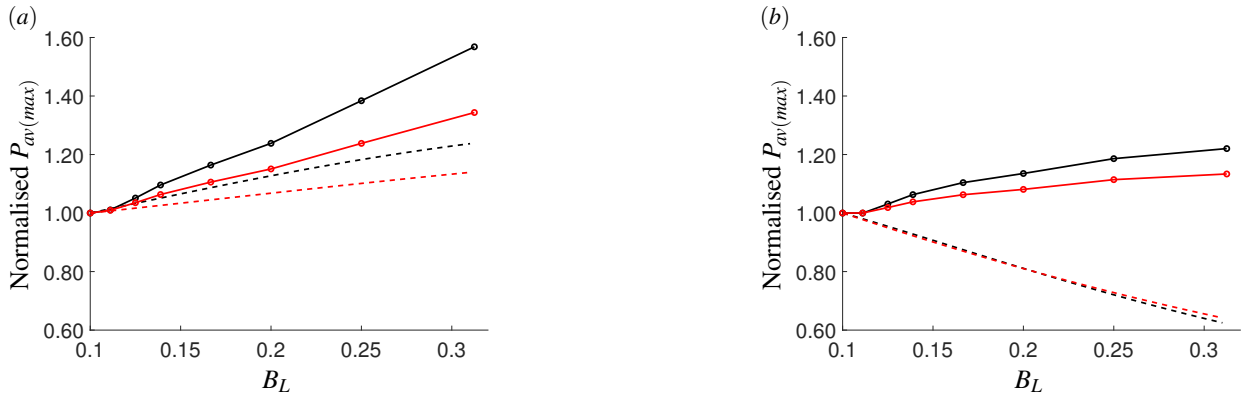

FIGURE 8: Numerically (solid lines connecting dots) and analytically (dashed lines) predicted variations in the potential for maximum available power, $P_{av(max)}$, enhancement with local blockage, B_L, for: (*a*) one row, and; (*b*) five rows of actuator discs (black) and tidal rotors (red) in oscillatory flow. (Colour online.)

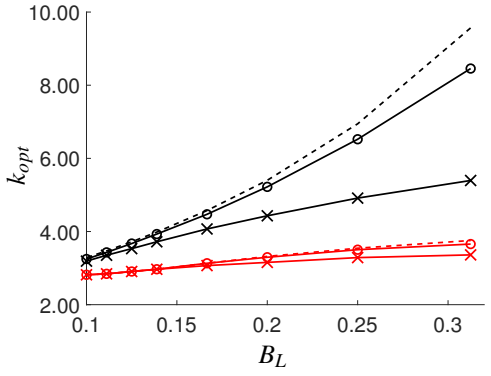

FIGURE 9: Variations in numerically (solid lines) predicted optimal local resistance coefficient, k_{opt}, for one row (circles) and five rows (crosses) of actuator discs (black) and tidal rotors (red) in oscillatory flow. Dashed lines show the corresponding variations for the individual turbines. (Colour online.)

idealised disc. Unlike for steady flow, however, the actuator disc is found to overestimate the performance of the tidal rotor by a greater amount when B_L is large, for both $N = 1$ and 5. This is because the highly idealised disc is able to apply considerably more thrust and produce, by means of this 'reversal boost', considerably more power.

CONCLUSIONS

In this paper, one-dimensional analytical and two-dimensional numerical models are used to explore the potential for local blockage effects to enhance the performance of turbines in tidal channels. Turbines are represented using the highly idealised actuator disc theory and the more realistic blade element momentum theory. The two-scale actuator disc theory of Nishino & Willden [1] is extended to incorporate tidal rotors, multiple rows of turbines, and following Willden et al. [19], coupled with an idealised theoretical model of channel-scale dynamics. In the case of steady flow, the two-scale theory is shown to

predict very well the results of the two-dimensional numerical model. In the case of oscillatory flow, however, numerical results show that the shorter and more highly blocked arrays produce considerably more power than predicted by the one-dimensional two-scale theory. These results support the findings of Bonar et al. [2], who showed that under certain oscillatory flow conditions, the power produced by a partial-width tidal turbine array can be much greater than predicted by two-scale theory. In oscillatory flow, the maximum available power is shown to increase with increasing local blockage, a finding which is consistent with the work of Bonar et al. [2]. Interestingly, this result is also found using a large number of turbine rows and a more advanced low-order turbine model. The effects of local blockage are shown to be less pronounced for the more realistic tidal rotor than for the highly idealised actuator disc, and in the case of a large number of turbine rows. In all oscillatory flow cases considered, however, the results show that considerably more power is available to the shorter and more highly blocked turbine arrays.

This study aims to provide new insights into the effects of local blockage on the performance of turbines in tidal channels, and further assess the potential for existing theoretical models to capture these effects. It is hoped that the present results will assist marine energy developers in selecting suitable models with which to determine optimal arrangements for tidal turbines and calculate the maximum available power. Further insights into the effects of local blockage on array performance may be achieved by considering different steady and oscillatory flow regimes, using, for instance, different values of channel bed roughness coefficient and tidal forcing amplitude. Array performance may also be improved by considering different rotor designs, or adopting time-varying turbine tuning [e.g. 27] or variable-pitch rotor control strategies [e.g. 16].

Acknowledgements

The authors wish to thank to Bowen Cao for providing invaluable assistance in the preparation of this article.

REFERENCES

[1] Nishino, T. & Willden, R.H.J. The efficiency of an array of tidal turbines partially blocking a wide channel. *J. Fluid Mech.*, 708: 596–606, 2012.

[2] Bonar, P.A.J., Chen, L., Schnabl, A.M., Venugopal, V., Borthwick, A.G.L., & Adcock, T.A.A. On the arrangement of tidal turbines in rough and oscillatory channel flow. *J. Fluid Mech.*, 865:790–810, 2019.

[3] Funke, S.W., Farrell, P.E., & Piggott, M.D. Tidal turbine array optimisation using the adjoint approach. *Renew. Energy*, 63:658–673, 2014.

[4] Garrett, C. & Cummins, P. The efficiency of a turbine in a tidal channel. *J. Fluid Mech.*, 588:243–251, 2007.

[5] Garrett, C. & Cummins, P. The power potential of tidal currents in channels. *Proc. R. Soc. A*, 461(2060):2563–2572, 2005.

[6] Vogel, C.R., Willden, R.H.J., & Houlsby, G.T. Blade element momentum theory for a tidal turbine. *Ocean Engng*, 169:215–226, 2018.

[7] Adcock, T.A.A., Draper, S., Houlsby, G.T., Borthwick, A.G.L., & Serhadlıoğlu, S. The available power from tidal stream turbines in the Pentland Firth. *Proc. R. Soc. A*, 469(2157):20130072, 2013.

[8] Houlsby, G.T., Draper, S., & Oldfield, M.L.G. Application of linear momentum actuator disc theory to open channel flow. Tech. Rep. OUEL 2296/08, Department of Engineering Science, University of Oxford, 2008.

[9] Vennell, R. Tuning turbines in a tidal channel. *J. Fluid Mech.*, 663:253–267, 2010.

[10] Draper, S. and Nishino, T. Centred and staggered arrangements of tidal turbines. *J. Fluid Mech.*, 739:72–93, 2014.

[11] Draper, S., Nishino, T., Adcock, T.A.A., & Taylor, P.H. Performance of an ideal turbine in an inviscid shear flow. *J. Fluid Mech.*, 796:86–112, 2016.

[12] Whelan, J.I., Graham, J.M.R., & Peiró, J. A free-surface and blockage correction for tidal turbines. *J. Fluid Mech.*, 624:281–291, 2009.

[13] Nishino, T. & Willden, R.H.J. Effects of 3-D channel blockage and turbulent wake mixing on the limit of power extraction by tidal turbines. *Int. J. Heat Fluid Flow*, 37:123–135, 2012.

[14] Schluntz, J. & Willden, R.H.J. The effect of blockage on tidal turbine rotor design and performance. *Renew. Energy*, 81:432–441, 2015.

[15] Vogel, C.R. *Theoretical limits to tidal stream energy extraction*. DPhil thesis, University of Oxford, 2014.

[16] Chen, L., Bonar, P.A.J., Vogel, C.R., & Adcock, T.A.A. A note on the tuning of turbines in tidal channels. *Journal of Ocean Engineering and Marine Energy*. In press.

[17] Cao, B., Willden, R.H.J., & Vogel, C.R. Effects of blockage and freestream turbulence intensity on tidal rotor design and performance. In *Proceedings of the 3rd International Conference on Renewable Energies Offshore, Lisbon, Portugal*, 2018.

[18] Wimshurst, A. & Willden, R.H.J. Computational analysis of blockage designed tidal turbine rotors. In *Proceedings of the 2nd International Conference on Renewable Energies Offshore, Lisbon, Portugal*, 2016.

[19] Willden, R.H.J., Nishino, T., & Schluntz, J. Tidal stream energy: Designing for blockage. In *Proceedings of the 3rd Oxford Tidal Energy Workshop, Oxford, UK*, 2014.

[20] Gong, X., Li, Y., and Lin, Z. Effects of blockage, arrangement, and channel dynamics on performance of turbines in a tidal array. *J. Renew. Sust. Energy*, 10:014501, 2018.

[21] Kubatko, E.J., Westerink, J.J., & Dawson, C. *hp* discontinuous Galerkin methods for advection dominated problems in shallow water flow. *Comp. Meth. Appl. Mech. Engng*, 196(1–3):437–451, 2006.

[22] Kubatko, E.J., Bunya, S., Dawson, C., & Westerink, J.J. Dynamic *p*-adaptive Runge-Kutta discontinuous Galerkin methods for the shallow water equations. *Comp. Meth. Appl. Mech. Engng*, 198 (21–26):1766–1774, 2009.

[23] Draper, S., Houlsby, G.T., Oldfield, M.L.G., & Borthwick, A.G.L.

Modelling tidal energy extraction in a depth-averaged coastal domain. *IET Renew. Power Gen.*, 4(6):545–554, 2010.

[24] Draper, S., Stallard, T., Stansby, P., Way, S., & Adcock, T. Laboratory scale experiments and preliminary modelling to investigate basin scale tidal stream energy extraction. In *Proceedings of the 10th European Wave and Tidal Energy Conference, Aalborg, Denmark*, 2013.

[25] Schnabl, A.M., Moreira, T.M., Wood, D., Kubatko, E.J., Houlsby, G.T., & Adcock, T.A.A. Implementation of tidal stream turbines and tidal barrage structures in DG-SWEM. In *ASME 38th International Conference on Ocean, Offshore and Arctic Engineering, Glasgow, Scotland*, 2019.

[26] Soulsby, R. *Dynamics of marine sands: a manual for practical applications*. Thomas Telford Publications, 1997.

[27] Vennell, R. & Adcock, T.A.A. Energy storage inherent in large tidal turbine farms. *Proc. R. Soc. A*, 470(2166):20130580, 2014.

[28] Perez-Campos, E. & Nishino, T. Numerical validation of the two-scale actuator disc theory for marine turbine arrays. In *Proceedings of the 11th European Wave and Tidal Energy Conference, Nantes, France*, 2015.

[29] Divett, T., Vennell, R., & Stevens, C. Channel scale optimisation of large tidal turbine arrays in packed rows using large eddy simulations with adaptive mesh. In *Proceedings of the 2nd Asian Wave and Tidal Energy Conference, Tokyo, Japan*, 2014.